Dimer structure of an interfacially impaired phosphatidylinositol-specific phospholipase C

Authors: C. Shao, Xiaomeng Shi, Hania Wehbi, Carlo Zambonelli, J.F. Head, B.A. Seaton, Mary F. Roberts

Published in *Journal of Biological Chemistry*, vol. 282, no. 12, pp. 9228-9235, 2007

THE JOURNAL OF BIOLOGICAL CHEMISTRY VOL. 282, NO. 12, pp. 9228–9235, March 23, 2007

Dimer Structure of an Interfacially Impaired Phosphatidylinositol-specific Phospholipase C*

Received for publication, November 27, 2006, and in revised form, January 5, 2007 Published, JBC Papers in Press, January 9, 2007, DOI 10.1074/jbc.M610918200

Chenghua Shao[‡], Xiaomeng Shi[§], Hania Wehbi[§], Carlo Zambonelli[§], James F. Head[‡], Barbara A. Seaton[‡], and Mary F. Roberts[§1]

From [§]Boston College, Chestnut Hill, Massachusetts 02467 and [‡]Boston University School of Medicine, Boston, Massachusetts 02118

The crystal structure of the W47A/W242A mutant of phosphatidylinositol-specific phospholipase C (PI-PLC) from *Bacillus thuringiensis* has been solved to 1.8 Å resolution. The W47A/W242A mutant is an interfacially challenged enzyme, and it has been proposed that one or both tryptophan side chains serve as membrane interfacial anchors (Feng, J., Wehbi, H., and Roberts, M. F. (2002) *J. Biol. Chem.* 277, 19867–19875). The crystal structure supports this hypothesis. Relative to the crystal structure of the closely related (97% identity) wild-type PI-PLC from *Bacillus cereus*, significant conformational differences occur at the membrane-binding interfacial region rather than the active site. The Trp → Ala mutations not only remove the membrane-partitioning aromatic side chains but also perturb the conformations of the so-called helix B and rim loop regions, both of which are implicated in interfacial binding. The crystal structure also reveals a homodimer, the first such observation for a bacterial PI-PLC, with pseudo-2-fold symmetry. The symmetric dimer interface is stabilized by hydrophobic and hydrogen-bonding interactions, contributed primarily by a central swath of aromatic residues arranged in a quasiherringbone pattern. Evidence that interfacially active wild-type PI-PLC enzymes may dimerize in the presence of phosphatidylcholine vesicles is provided by fluorescence quenching of PI-PLC mutants with pyrene-labeled cysteine residues. The combined data suggest that wild-type PI-PLC can form similar homodimers, anchored to the interface by the tryptophan and neighboring membrane-partitioning residues.

Phosphatidylinositol-specific phospholipase C (PI-PLC)[2] enzymes catalyze the specific cleavage of the *sn*-3-phosphodiester bond in phosphatidylinositol (PI) and phosphoinositides. PI hydrolysis occurs in two sequential reactions (1–3): (i) an intramolecular phosphotransferase reaction at a phospholipid/aggregate surface to produce diacylglycerol and water-soluble 1,2-cyclic inositol phosphate (cIP) (or cIP_x in the case of a phosphoinositide substrate), followed by (ii) a phosphodiesterase reaction where water-soluble cIP is hydrolyzed to inositol-1-phosphate. Since their substrate is presented in an interface, their activity can often be modulated by the composition of the interface. Eukaryotic PI-PLCs, as critical components of phosphatidylinositol-mediated signaling pathways (4, 5), have multiple domains for regulation of enzyme activity both by regulating partitioning to membranes and by allosteric effects on catalysis, and these are often hard to separate. However, the much smaller bacterial PI-PLC enzymes are secreted, single domain proteins whose crystal structures (6–8) resemble the catalytic domain of $PLC\delta_1$, the only mammalian PI-PLC for which there is a structure (9–11). The molecular topology is that of a distorted TIM barrel. Around the barrel rim, there are regions where hydrophobic side chains are exposed to solvent. The structural similarity of the bacterial PI-PLC to the mammalian catalytic domain and similar kinetic features (12–14) suggest that the smaller enzyme can provide a simple model for understanding how different interfaces modulate catalysis.

Previous work has shown that the PI-PLC from *Bacillus cereus* or *Bacillus thuringiensis* not only prefers micellar to monomeric substrate (15) but is also activated by binding to phosphatidylcholine (PC) interfaces (2, 16, 17). The binding has an allosteric effect on the enzyme, since it increases k_{cat} and decreases K_m for hydrolysis of the soluble substrate cIP. PC also alters kinetic parameters for PI cleavage (18). Hendrickson and Hendrickson (19) showed that resonance energy transfer occurs between one (or more) of the seven Trp residues in *B. cereus* PI-PLC and a dansyl group at the terminus of the *sn*-1 alkyl chain of PC dispersed in a hexadecylphosphorylcholine aggregate. This indicates that there must be some direct partitioning of the protein into the membrane, although it does not indicate the segment(s) of the protein involved. The rim of the ($\beta\alpha$)-barrel above the active site of bacterial PI-PLC has a short helix B and one particular loop (^{236}SSGGTAWNS^{244}) that show an unusual clustering of hydrophobic amino acids that are fully exposed to solvent. These two structural units contribute to the binding of the PC activator with both Trp^{47} and Trp^{242} important for the enzyme to bind to interfaces (both activating zwitterionic (PC) and substrate anionic surfaces) (20, 21). The W47A/W242A mutant showed minimal activation of cIP, dramatically reduced PI cleavage, and virtually no binding to PC interfaces, vesicles, or micelles.

In this work, we report the crystal structure of the W47A/W242A mutant (double mutant of W47A and W242A) PI-PLC.

* This work was supported by National Institutes of Health Grant GM60418 (to M. F. R.). The costs of publication of this article were defrayed in part by the payment of page charges. This article must therefore be hereby marked "*advertisement*" in accordance with 18 U.S.C. Section 1734 solely to indicate this fact.

[1] To whom correspondence should be addressed: Merkert Chemistry Center, Boston College, Chestnut Hill MA 02465. Tel.: 617-552-3616; Fax: 617-552-2705; E-mail: mary.roberts@bc.edu.

[2] The abbreviations used are: PI-PLC, phosphatidylinositol-specific phospholipase C; PI, phosphatidylinositol; PC, phosphatidylcholine; POPC, 1-palmitoyl-2-oleoyl-PC; diC_7PC, diheptanoyl-PC; cIP, 1,2-cyclic inositol phosphate; r.m.s., root mean square.

TABLE 1

PI-PLC cysteine mutant and pyrene adduct phosphotransferase-specific activities and apparent dissociation constants (POPC small unilamellar vesicles)

PI-PLC	Specific activity[a]	nK_d[b]
	$\mu mol\ min^{-1}\ mg^{-1}$	μM
Wild type	900	64 ± 3[c]
W47/242A	140	>25,000[c]
Y57C	850	59 ± 19
Y57C-pyr	810	70 ± 8
W242C	815	200 ± 15
W242C-pyr	1050	125 ± 20
S250C	1480	71 ± 25
S250C-pyr	1100	43 ± 10
W280C	270	66 ± 12
W280C-pyr	325	40 ± 5

[a] The phosphotransferase activities were measured at 28 °C towards 8 mM PI solubilized in 32 mM diC_7PC, pH 7.5. Errors in specific activities determined by ^{31}P were <20%.
[b] An apparent dissociation constant extracted from analyzing binding of these PLC enzymes to vesicles using a Langmuir adsorption model (29).
[c] From Wehbi *et al.* (29).

TABLE 2

Crystallographic data and refinement statistics

Parameter	Value
Diffraction data	
Wavelength (Å)	1.1000
Resolution (Å)	1.84
Space group	$P2_12_12_1$
Unit cell dimensions (Å)	$a = 64.4, b = 70.0, c = 154.1$
No. of unique reflections	60,615
Completeness[a] (%)	98.8 (90.6)
Redundancy	4.4
R_{merge}[b] (%)	4.2 (15.8)
Refinement	
Resolution range (Å)	50-1.84
R_{cryst}[c]	0.1853
R_{free}[d]	0.2148
No. of protein atoms	4806
No. of water molecules	576
No. of atoms total	5382
r.m.s. deviation bond angles (degrees)	1.2971
r.m.s. deviation bond lengths (Å)	0.0049
Mean $\langle B \rangle$ overall (Å^2)	23.3
Mean $\langle B \rangle$ protein (Å^2)	22.1
Ramachandran regions (% residues)	
Most favored	85.2
Additional allowed	14.4
Generously allowed	0.4[e]
Disallowed	0.0

[a] Completeness reported for all reflections and for the highest resolution shell (values in parenthesis).
[b] R_{merge} reported for all reflections and for the highest-resolution shell (values in parenthesis). $R_{merge} = \Sigma|I_i - \langle I \rangle|/\Sigma I_i$, where I_i is the intensity of an individual reflection, and $\langle I \rangle$ is the mean intensity of that reflection.
[c] $R_{cryst} = \Sigma\frac{1}{2}|F_p| - |F_c\frac{1}{2}|/\Sigma|F_p|$, where $|F_c|$ and $|F_p|$ are the calculated and observed structure factors, respectively.
[d] R_{free} as defined by Brunger *et al.* (27).
[e] 0.4% residues in the generously allowed region correspond to Glu^{146} from both monomers in the asymmetric unit, as observed previously (31).

Although the overall structure and the active site of this mutant are very similar to that in the structure of the PI-PLC from *B. cereus* (6), helix B has been disrupted, and the orientation of the loop 236–244 has shifted. More unexpectedly, this mutant protein crystallized as a dimer in the asymmetric unit, the first time a bacterial PI-PLC oligomer has been observed. Complementary binding components and intermolecular interactions (both hydrophobic and hydrophilic) at the dimer interface suggest that the dimer is as stable as those observed in other, naturally occurring protein-protein complexes (22). Fluorescence quenching assays of various PI-PLC constructs with fluorophores introduced in the region of the dimer interface strongly support the idea that binding to PC interfaces promotes formation of the dimer.

EXPERIMENTAL PROCEDURES

PI-PLC Expression, Purification, and Modification—A plasmid containing the *B. thuringiensis* PI-PLC gene was transformed into *Escherichia coli* BL21-Codonplus (DE3)-RIL cells (Stratagene). Overexpression and purification of W47A/W242A followed procedures described previously (20). Several cysteine mutants (Y57C, W242C, S250C, and W280C) of PI-PLC were prepared (using QuikChange™ mutagenesis) to introduce extrinsic fluorophores into the protein; all mutated genes were sequenced to confirm that the desired mutation was introduced. These mutants expressed well in *E. coli*; purification to >90% as monitored by SDS-PAGE was achieved by chromatography on a Q-Sepharose fast flow column followed by a phenyl-Sepharose column as described for the recombinant enzyme (20). The phosphotransferase reaction of PI-PLC cysteine mutants was monitored by following cIP production with ^{31}P NMR spectroscopy as described previously (1, 2, 20). Assay conditions included 8 mM PI solubilized in 32 mM diC_7PC micelles in 50 mM HEPES, pH 7.5, at 28 °C. Most of the PI-PLC cysteine mutants had phosphotransferase-specific activities comparable with that for recombinant PI-PLC (Table 1). The one exception was W280C, which was 30% that of the control. The Cys mutants, 1.5–3.0 mg/ml (50–100 μM) in 50 mM Tris-HCl, pH 7.3, were derivatized at room temperature with *N*-(1-pyrene)iodoacetamide added dropwise from a 15 mM stock solution in dimethylformamide made immediately prior to use and protected from light. The reaction was allowed to proceed for 2 h at room temperature in the dark. When the reaction was completed, an excess of mercaptoethanol was added to consume excess thiol-reactive reagent. The reaction product was then extensively dialyzed at 4 °C in 50 mM Tris, pH 7.5. Less than 10% Cys remained as monitored by Ellman's reagent (23). Protein solutions were concentrated using Millipore Centraplus 10 filters; protein concentrations were determined by Lowry or Bradford assays.

X-ray Crystallography—Crystals of PI-PLC W47A/W242A mutant were grown at 17 °C by vapor diffusion in hanging drop against a reservoir solution containing 15% 2-methyl-2,4-pentanediol, 16% polyethylene glycol 400, and 0.1 M citrate buffer at pH 5.4. Crystallographic data were collected at the Brookhaven National Laboratory Synchrotron X8C beam line. Crystals were directly cooled to 80–100 K by vapor nitrogen stream prior to collection. Data were indexed, integrated, and scaled using the DENZO and SCALEPACK software packages (24).

Phases were provided by molecular replacement using the program EPMR (25) and previous structures of wild type PI-PLC from *B. cereus* (Protein Data Bank entry 1PTD) as a starting model (6). Model-building and refinement steps were carried out using O (26) and CNS (27), respectively. Individual B-factors were refined for all atoms. Data collection and refinement statistics of the crystallization work are presented in Table 2. The PDB code for this structure is 2OR2. Crystallographic figures were all made through Pymol (28).

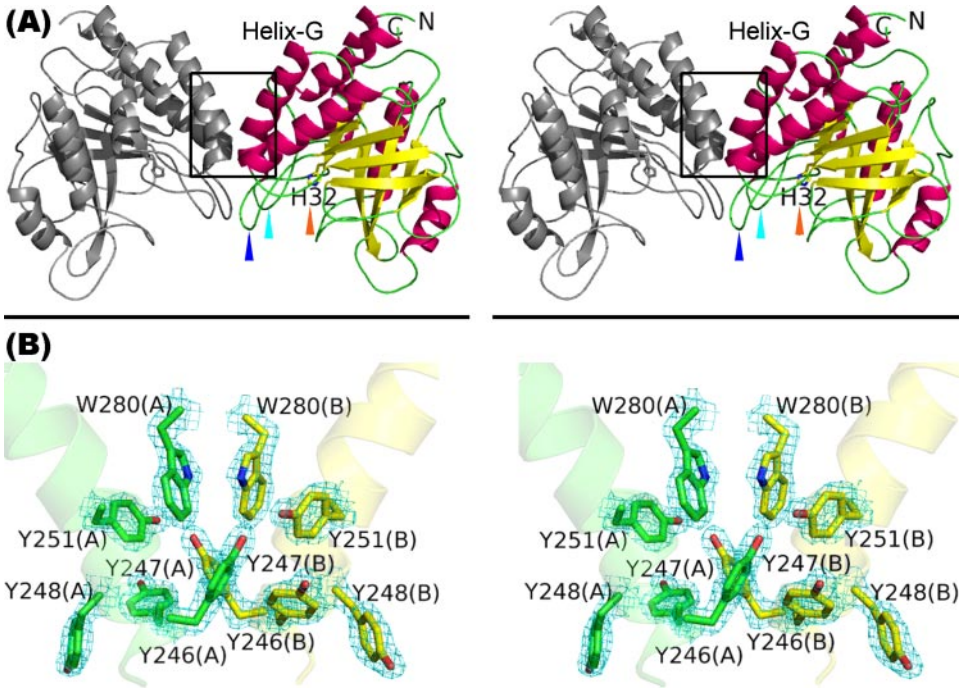

FIGURE 1. **Structure of the PI-PLC W47A/W242A mutant dimer from *B. thuringiensis* shown in divergent (wall-eyed) stereo view.** *A*, *ribbon diagram* of the dimer. N and C termini are labeled; the *boxed region* indicates the dimer interface (shown in detail in Fig. 1*B*). The active site residue His^{32} is shown as a *stick model*, and the *orange arrow* points to the location of the active site. Residues Ile^{43}–Gly^{48}, which form helix B in the *B. cereus* structure but not in the mutant structure, and the rim loop region (Ser^{236}–Ser^{244}) are indicated by *cyan* or *blue arrows*, respectively. *B*, aromatic residues (*stick representation*; the subunits to which the residues belong are indicated with *A* or *B* in *parentheses*) located within the hydrophobic core of the symmetric dimer interface. *Lightly colored helices* are the N-terminal parts of helix G from both monomers. Shown in the cyan network is the electron density from the omit map omitting Tyr^{246}, Tyr^{247}, Tyr^{248}, Tyr^{251}, and Trp^{280} from both subunits and contoured at 1.2 σ.

TABLE 3
Dimer interface descriptive parameters

Protein interface parameter[a]	Value
Interface-accessible surface area (Å^2)	884.36
Percentage of interface-accessible surface area	7.52
Planarity	2.50
Length, Breadth (Å)	27.31, 25.78
No. of residues involved in binding[b]	27 (9.1%)
Percentage of polar atoms in interface	35.67
Percentage of nonpolar atoms in interface	64.30
Hydrogen bonds	10
Gap volume	4531.48
Gap volume index	2.56

[a] Calculation was made through the protein-protein interactions server at the biomolecular structure and modeling group of London's Global University. The calculation on the server, including parameter definitions, was based on Jones and Thornton (22, 40).
[b] Total number and percentage (in parentheses) of residues includes contributions from either monomer.

POPC Vesicle Binding Assay—A simple binding assay based on centrifugation (29) was used to characterize the binding of W242C and pyrene-modified W242C and other Cys mutants to sonicated vesicles of 1-palmitoyl-2-oleoyl-phosphatidylcholine (POPC) obtained from Avanti Polar Lipids. Vesicle-bound enzyme (E_B) was separated from free enzyme (E_F) using an Amicon Centricon-100 filter. The filtrate, containing free enzyme, was lyophilized and analyzed by SDS-PAGE. Binding was analyzed using a Langmuir adsorption isotherm (29, 30), where n is the number of lipid molecules in the surface to which each enzyme molecule is assumed to bind, and K_d is the dissociation constant for the binding site composed of n lipids. The product "nK_d" provides an apparent dissociation constant for comparison of the different PI-PLC proteins.

Fluorescence Spectroscopy—The accessibility of a given pyrene-labeled PI-PLC to the water-soluble quenching agent acrylamide was studied in the absence and presence of POPC vesicles prepared by sonication. For quenching experiments, conditions included 0.05 mg/ml (1.4 μM) protein and 1 mM POPC vesicles prepared by sonication in 50 mM Tris-HCl, pH 7.0. Labeled PI-PLC fluorescence spectra as a function of added acrylamide (from a 2 M stock solution) were obtained with either a Shimadzu RF5000U spectrofluorometer or a Fluorolog R-3 spectrofluorometer with excitation at 334 nm and emission monitored at 383 nm.

RESULTS

Crystal Structure of the W47A/W242A Mutant of PI-PLC—The *B. thuringiensis* PI-PLC W47A/W242A mutant crystallized in the $P2_12_12_1$ space group with two monomers in the asymmetric unit (Fig. 1). The two monomers are structurally very similar to each other, with r.m.s. deviations of 0.291 Å (main chain) and 0.549 Å (overall). Each monomer folds as an incomplete $(\beta\alpha)_8$-barrel in which the inner layer of the barrel is composed of eight β-strands, surrounded by the six α-helices of the outer layer (the two helices paired with strands IV and V are absent in the bacterial PI-PLC enzymes). In the W47A/W242A crystal structure, the two C-terminal residues of PI-PLC, Lys^{297} and Glu^{298}, are omitted due to lack of electron density. The subunit interface of the pseudo-2-fold symmetric dimer is composed of the 27 residues (9.1% of the total number of residues) from one monomer and the same 27 residues from another. These residues are mostly contributed from helix G, helix B, and the rim loop. The dimer interface is ~27 Å in length and 26 Å in width, with an accessible surface area of 884 Å^2, covering 7.5% of the surface area of each monomer (Table 3). The contacts between the two monomers are primarily hydrophobic, with 64.3% contributed by nonpolar interacting atoms. These are stabilized further by 10 intermolecular hydrogen bonds (Tables 4 and 5). The dimer interface reveals a striking surface complementarity in which the most significant interactions are contributed by a cluster of aromatic residues. The aromatic rings of Tyr^{246}, Tyr^{247}, Tyr^{248}, and Tyr^{251} from helix G and Trp^{280} pack into a quasiherringbone pattern forming a hydrophobic core within the interface (Fig. 1*B*). The rings of Tyr^{246}, Tyr^{247}, and Tyr^{251} make strong hydrophobic interactions with residues from the other monomer. Tyr^{248} and Trp^{280}

TABLE 4

Major hydrophobic interactions of aromatic residues at the dimer interface. Intramolecular interactions (within 4 Å) are explicitly named for only one monomer but apply equally to both

Chain	Residue	Chain	Residue
A	Pro^{42}	B	Tyr^{247}
A	Pro^{42}	B	Tyr^{248}
A	Tyr^{246}	A	Trp^{280}
A	Tyr^{246}	B	Tyr^{246}
A	Tyr^{246}	B	Tyr^{247}
A	Tyr^{246}	B	Tyr^{251}
A	Tyr^{247}	A	Tyr^{248}
A	Tyr^{247}	A	Tyr^{251}
A	Tyr^{247}	B	Pro^{42}
A	Tyr^{247}	B	Tyr^{246}
A	Tyr^{248}	B	Pro^{42}
A	Tyr^{251}	B	Tyr^{246}
A	Pro^{254}	A	Trp^{280}

TABLE 5

Intermolecular hydrogen bonds formed at the dimer interface

Monomer A		Monomer B	
Residue	Atom	Residue	Atom
Gln^{45}	Oϵ1	Gly^{239}	N
Glu^{52}	Oϵ2	Tyr^{247}	Oη
Glu^{52}	Oϵ2	Tyr^{251}	Oη
Gly^{239}	N	Gln^{45}	Oϵ1
Tyr^{246}	Oη	Ser^{250}	Oγ
Tyr^{247}	Oη	Glu^{52}	Oϵ2
Ser^{250}	Oγ	Tyr^{246}	Oη
Ser^{250}	O	Lys^{279}	Nζ
Tyr^{251}	Oη	Glu^{52}	Oϵ2
Lys^{279}	Nζ	Ser^{250}	O

remain confined to their own respective monomers and provide stabilization for the hydrophobic core boundary.

The effects of the W47A/W242A mutation on PI-PLC structure and function can be seen by comparison with other PI-PLC crystal structures. The amino acid sequence of *B. thuringiensis* PI-PLC is similar to that of the *B. cereus* enzyme, with 97% sequence identity. The only significant differences between the crystal structures of the *B. cereus* wild type (Protein Data Bank entry 1PTD) (6) and *B. thuringiensis* W47A/W242A mutant enzymes are localized to the so-called helix B (Ile^{43}–Gly^{48}) and rim loop (Ser^{236}–Ser^{244}) regions (Fig. 2). These regions, and their Trp residues in particular, have been implicated in binding of the protein to PC bilayers, since replacement of either Trp^{47} or Trp^{242} with alanine dramatically reduces the affinity of the protein for PC bilayers by an amount comparable with what would be expected if a membrane-soluble Trp side chain were replaced by the much less hydrophobic methyl group of alanine (20, 21). The "helix B" region of the W47A/W242A mutant adopts an irregular loop conformation rather than the α-helix observed in wild type PI-PLC. The overall shape of the rim loop is similar in the two enzymes, but in the mutant, the loop shifts positionally closer to the lower center of the (βα)-barrel, which changes the relative orientation between the rim loop and helix B. In the wild-type enzyme, the closest Cα-Cα distance between the rim loop and B helix is 5.1 Å from Val^{46} to Gly^{239}, whereas the distance between Val^{46} and Gly^{239} is changed to 13.5 Å in the mutant enzyme. When residues from the helix B and rim loop are omitted from the superposition calculation, the main-chain r.m.s. deviation falls from 1.305 to 0.514 Å, confirming that significant structural differences are confined to these two regions. Comparison of the crystal structures of *B. thuringiensis* PI-PLC mutants W47A/W242A and R69D (Protein Data Bank entry 1T6M) (31), which contains a metal ion site introduced into the active site, produces similar results: main-chain r.m.s. deviation values fall from 1.352 Å (all residues) to 0.586 Å with residues at helix B and the rim loop omitted. On the other hand, the main-chain r.m.s. deviation between *B. cereus* wild-type and *B. thuringiensis* R69D mutant PI-PLC structures is 0.653 Å for all residues, indicating that despite the species and sequence differences, they retain highly similar conformations in the absence of the W47A/W242A mutation. Of particular note is the observation that the W47A/W242A mutation has no observable effect on active site geometry, which in the mutant aligns closely with the active sites of *B. cereus* wild-type PI-PLC, with or without inhibitors. The r.m.s. deviation for the 13 active site residues (as defined in Ref. 6) is 0.564 Å (all atoms). These comparisons reveal that significant structural effects of the W47A/W242A mutation are limited to the helix B and rim loop regions, leaving the active site geometry unaltered and capable of catalysis.

Acrylamide Quenching of PI-PLC Mutants—To evaluate whether the PI-PLC dimer can be detected in an interfacial environment, we initially considered chemical cross-linking (32); however, a dearth of reactive functionalities in the vicinity of the dimer interface proved to be a serious drawback for this approach. We have chosen to use instead an extrinsic fluorescence approach to evaluate solvent accessibility at selected residue positions in the presence or absence of a PC interface. Since cysteine residues do not occur naturally in PI-PLC, we introduced cysteine residues at positions near the observed dimer interface. Each cysteine-containing mutant was derivatized with *N*-(1-pyrene)iodoacetamide to introduce a pyrene moiety that served as a probe to evaluate accessibility to acrylamide at that position. Acrylamide has no tendency to partition into the interior of the bilayer or the protein core; nor does it concentrate at the bilayer surface. Acrylamide quenching thus reports on surface exposure of fluorescence-labeled residues. Cysteine residues were substituted through mutagenesis for Trp^{242} (a loop rim residue that has been implicated in PC membrane partitioning), Ser^{250} (located centrally at the dimer interface and proximal to the rim loop), and Trp^{280} (located in the dimer interface but distant from the barrel rim). Tyr^{57}, a surface residue that is not situated at the putative dimer or membrane interface, was included as a control. As shown in Table 1, all Cys mutants but W242C exhibited nK_d values (for POPC small unilamellar vesicles) comparable with the 64 ± 3 μM previously obtained for recombinant PI-PLC (29). Previous work showed that W242A lost significant affinity for PC with an apparent dissociation constant of 8600 ± 600 μM (20). Interestingly, the W242C nK_d value, 200 ± 15 μM, was about 40-fold lower than for W242A and only about 3-fold higher than recombinant PI-PLC. Introduction of the pyrene moiety at this position enhanced its affinity for PC vesicles with nK_d reduced to 125 ± 20 μM (2-fold higher than wild type). Thus, all pyrene-labeled PI-PLC enzymes bound effectively to PC vesicles. They also exhibited specific activities toward PI solubilized in diC_7PC micelles comparable with recombinant wild-type PI-PLC and much higher than for W47A/W242A (Table 1).

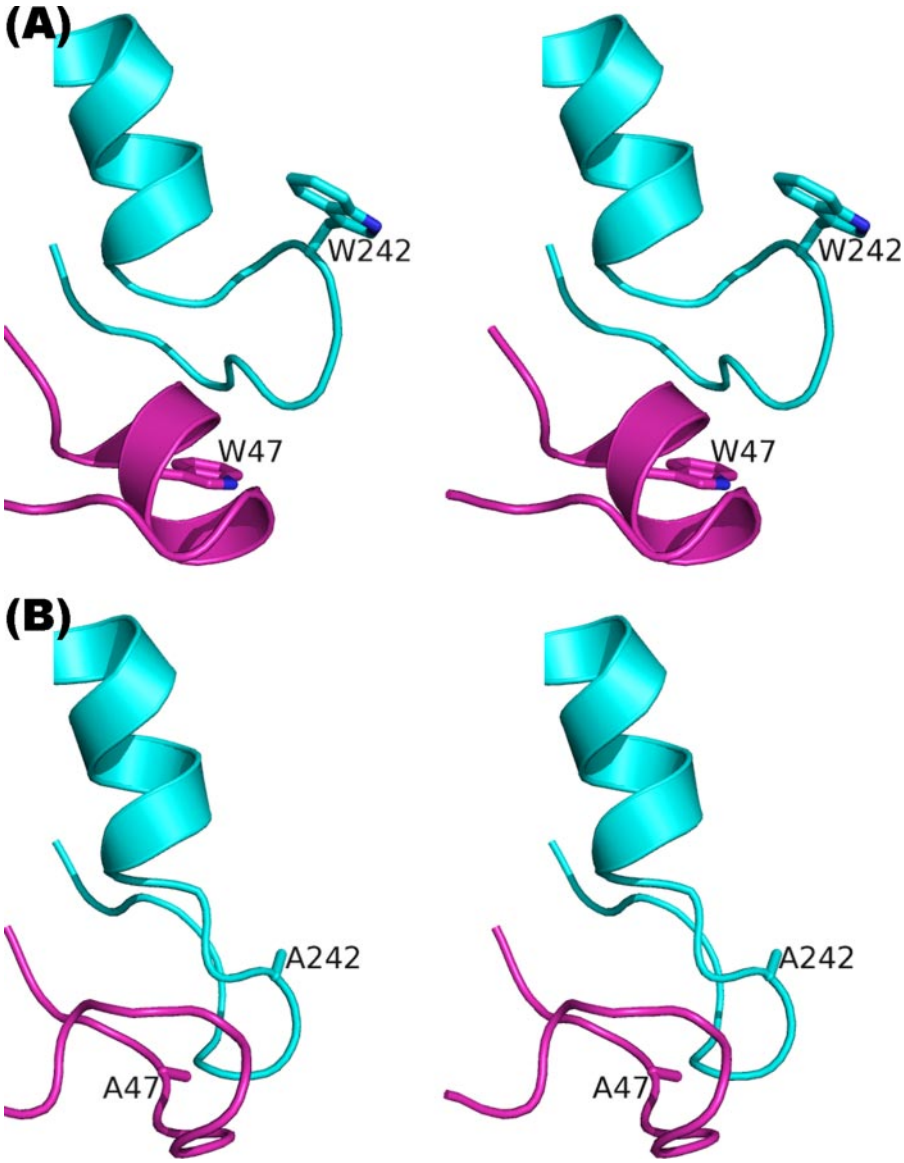

FIGURE 2. ***Ribbon representations*** **of the helix B region (*magenta*) and rim loop region (together with the N terminus of helix G) (*cyan*) of wild-type *B. cereus* PI-PLC (Protein Data Bank entry 1PTD (6)) (*A*) and *B. thuringiensis* W47A/W242A mutant PI-PLC (*B*).** Side chains at positions 47 and 242 are shown as *stick representations* in both *A* and *B*.

In a noninterfacial environment, the pyrene probes attached to Y57C, W242C, S250C, and W280C could be quenched by acrylamide, consistent with substantial solvent exposure for these pyrene labels (Fig. 3*A*). It was further observed that all of the pyrene-labeled PI-PLC mutants except Y57C exhibited nonlinear Stern-Volmer plots. Assuming collisional quenching, this nonlinearity could be explained by two pools of the pyrene: one accessible to quencher (*e.g.* monomer) and the other inaccessible (*e.g.* dimer). If one uses a modified Stern-Volmer equation ($F_o/\Delta F = 1/(f_a K_a[Q]) + 1/f_a$, where f_a is the fraction of fluorophore accessible to quenching and K_a is a quenching constant) (33) to fit the data, f_a values were 0.56, 0.37, and 0.29 for pyrene attached to W242C, S250C, and W280C in the absence of an interface, and the Stern-Volmer quenching constants (K_v) for the accessible pyrene-labeled proteins were >3 (Table 1). Previous studies have shown that wild-type PI-PLC exists predominantly as a monomer in solution (17). However, it is possible that introducing the large pyrene probe makes the dimer interface region more hydrophobic in solution, thus shifting the monomer-dimer equilibrium for the derivatized proteins and giving rise to two fluorophore populations. In contrast, the presence of a phospholipid interface (POPC vesicles) provided nearly complete protection from acrylamide quenching (values of K_v with the Stern-Volmer equation yielded values of $<0.5\ \text{M}^{-1}$ for all mutants but Y57C) (Fig. 3*B*). K_v only decreased a small amount for Y57C-pyrene in the presence of vesicles, indicating that this residue is exposed to solvent whether or not the protein is bound to a vesicle.

None of the pyrene-labeled proteins showed any excimer bands either free in solution or when bound to PC surfaces, even those attached to residues near the dimer interface. The stacked orientation of two pyrene rings is critical for excimer formation. If each pyrene ring in the dimer adopts a conformation compatible with the herringbone pattern observed at the interface, there would not be efficient excimer formation.

DISCUSSION

Previous kinetic studies have established that the *B. thuringiensis* PI-PLC W47A/W242A mutant is an interfacially impaired enzyme that no longer binds well to activating PC interfaces (20). Removal of these two tryptophan residues, singly or together, dramatically increases the apparent K_D (or nK_d in a Langmuir adsorption model for binding (29)) for partitioning of the enzyme onto PC vesicles, and the magnitude of the change is consistent with the change in free energy for removing a group that partitions into the PC membrane. X-ray crystallography was used to investigate protein structural changes that might be associated with the W47A/W242A mutation and to determine whether such changes might occur in the active site, resulting in a lower k_{cat}. The crystal structure demonstrates that the *B. thuringiensis* PI-PLC W47A/W242A mutant retains the overall ($\beta\alpha$)-barrel structure (Fig. 1) observed in the crystal structure of *B. cereus* wild-type PI-PLC (6). Crystal structures of wild-type PI-PLC complexes with inositol have established that the active site is located inside the β-barrel, and the lower barrel rim allows the substrate entry from the membrane bilayer. Comparison of the

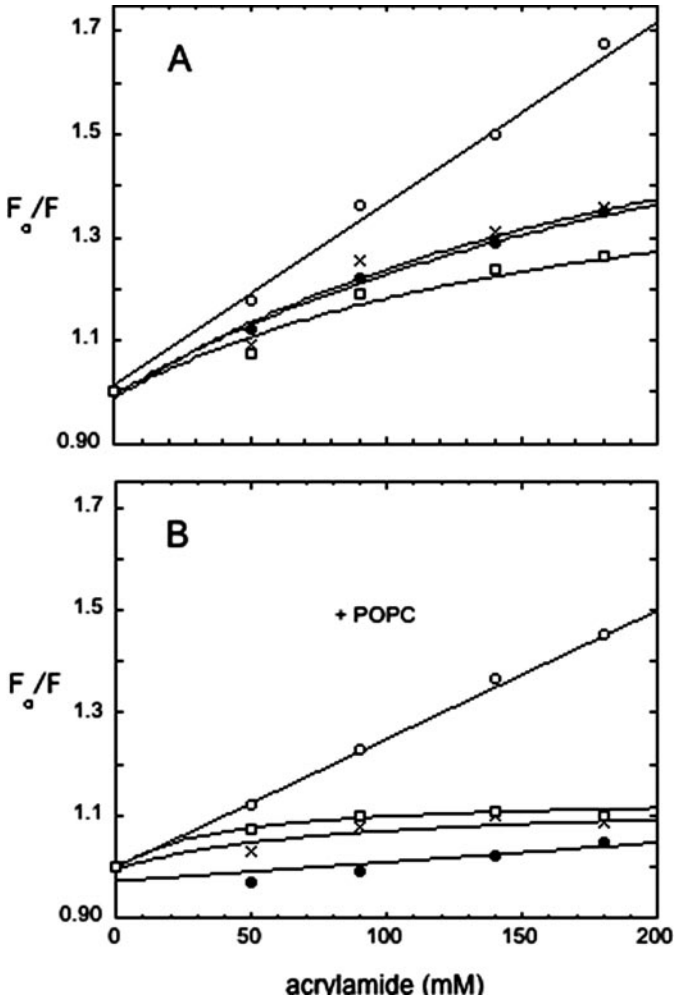

FIGURE 3. **Acrylamide quenching of pyrene-labeled PI-PLC (0.05 mg/ml) in the absence (*A*) and presence (*B*) of 1 mM POPC small unilamellar vesicles.** ○, Y57C-pyr; ●, W242C-pyr; ×, S250C-pyr; □, W280C-pyr.

wild-type and W47A/W242A mutant structures indicates no significant structural differences between the active sites. However, the W47A/W242A mutant reveals a major conformational change in two regions that have been implicated in membrane binding (20, 21). The W47A/W242A mutation perturbs the helix B region, which in wild-type PI-PLC forms a short α-helix (residues Ile^{43}–Gly^{48}) that has been proposed to partially insert into membranes (21, 29). In wild-type PI-PLC, this helix orients the side chains of Ile^{43}, Val^{46}, and Trp^{47} so that they pack together and form a plug that extends outwards toward solvent, thus forming a hydrophobic protrusion from the protein surface. This hydrophobic protrusion occurs near the lower rim entrance, where the protrusion could act to stabilize membrane binding and perhaps encourage the proper orientation of the β-barrel with respect to the interfacial surface. The W47A mutation disrupts the helical secondary structure, which in turn alters the relative orientation of these side chains. The Ile^{43} side chain becomes redirected into the protein core, and the Cα–Cα distance between residues 43 and 46 increases from 5.3 to 8.3 Å. These data are consistent with the premise that the decreased catalytic activity of the mutant is due primarily to the loss of its membrane binding capacity. Deficient membrane binding could alter the enzyme activity in various ways (*e.g.* reduction of enzyme-ligand contact or failure to induce an active site environment that promotes catalysis).

An unexpected feature to emerge from the present studies is the first crystallographic observation of a PI-PLC dimer. Dimers have been observed crystallographically for three other phospholipases (A, A_2, and the C-terminal tail of phospholipase C-β); however, the first two of these are structurally and functionally distinct from PI-PLC enzymes, and the last is an isolated domain. The outer membrane phospholipase A of Gram-negative bacteria is an integral β-barrel membrane protein that is active *in vitro* as a dimer (34). Dimerization depends on substrate and Ca^{2+} binding, and the complete active site requires dimer formation (35). The anion-assisted dimer of secreted phospholipase A_2 (36) forms a catalytically inactive enzyme. Avian phospholipase C-β, which possesses a fold unique to these enzymes, forms dimers that mediate interactions with G-proteins (37, 38). A recent report shows that an isoform of mammalian PI-PLC can also form homodimers (39). Although crystal structures of mammalian PLC-β have yet to be determined, the report implicated the involvement of the catalytic domain in the dimerization. Precedent thus exists for homodimerization in other phospholipases, despite the diversity in structural motifs and functional properties.

The dimer interface of *B. thuringiensis* W47A/W242A PI-PLC exhibits high complementarity, with a striking pseudo-2-fold symmetry in which aromatic side chains form an interdigitating core involving the same residues from each monomer. Such symmetry is observed frequently in macromolecular assemblies. In the W47A/W242A dimer, the monomers are oriented parallel to each other, such that the pseudo-2-fold axis of the dimer interface parallels the axes passing through the two β-barrels. This orientation for the monomers would preserve the interfacial active site accessibility for both. The 2-fold symmetry creates some curvature in the dimer (Fig. 1*A*), which may be consistent with the strong preference exhibited for small, highly curved unilamellar vesicles of PC compared with large, more planar bilayer vesicles (29). It is also possible that the dimer may reorient slightly to adopt a more planar shape on a membrane surface. Such a reorientation could be accommodated with only minor adjustments of the aromatic residues at the dimer interface.

The combined data suggest that PI-PLC from *B. cereus* and *B. thuringiensis* share an inherent ability to form dimers. The residues that comprise the dimer interface are conserved in PI-PLC from both species. In the wild-type PI-PLC crystal structure, these side chains are surface-accessible and available to participate in protein-protein interactions. Given the similarities between the enzymes, it is intriguing that the crystallographic dimer has been observed solely for the W47A/W242A mutant. The data herein suggest that the crystallization behavior is critically influenced by the local conformation of the B helix and barrel rim regions, particularly the Trp^{47} and Trp^{242} side chains. In the conformation observed in the *B. cereus* wild-type PI-PLC crystal structure, the hydrophobic protrusion from the B-helix extends outwards in an orientation that interferes with formation of the lower boundary of the dimer inter-

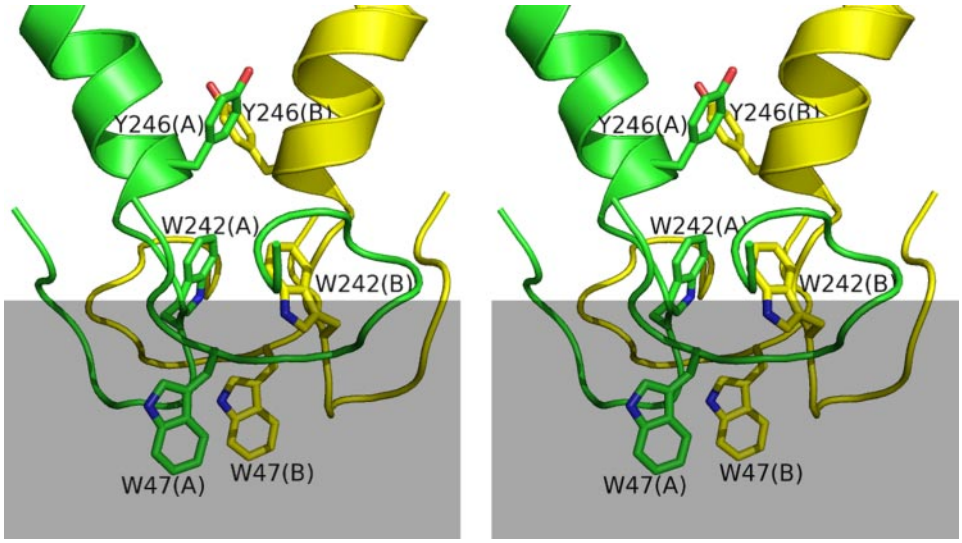

FIGURE 4. **Possible conformation (based on the W47A/W242A dimer structure) adopted by wild-type PI-PLC at the PC membrane interface (indicated by the *gray shadow*).** Subunits A and B are shown in *green* and *yellow*, respectively. Tyr^{246} side chains are included to indicate the orientation of the molecule similar to that shown in Fig. 1*B*.

face; the bulky tryptophan side chains prevent the requisite close intermolecular contacts observed in the dimer structure. However, these regions are conformationally mobile, and partitioning of the protrusion into the membrane could relieve the steric hindrance and permit dimerization. Indeed, in the W47A/W242A mutant, such a conformational transition is effected by the substitution of alanine for the bulky side chains of tryptophans 47 and 242. The double mutation brings the Cα–Cα distance between residues 47 and 242 in the same monomer 2.3 Å closer to each other. The distance between the Ala^{47}/Ala^{242} pair from one monomer to the other is also close, ~5 Å (Cα–Cα). These close distances are compatible with dimerization. One possible model for the dimer interface of wild-type PI-PLC, based on the W47A/W242A crystal structure, is shown in Fig. 4.

The fluorescence and crystallographic data are in agreement and together support a model in which dimer formation is promoted by membrane binding. When PI-PLC is free in solution and not membrane-associated, the corresponding fluorescence data demonstrate that all of the pyrene-labeled residues are exposed to solvent. The crystal structure of *B. cereus* wild-type PI-PLC shows that these same four residues are located at the protein surface. Since dimer formation, as seen in the crystal structure of *B. thuringiensis* W47A/W242A PI-PLC, would be expected to bury Ser^{250} and Trp^{280}, their significant solvent accessibility in solution is consistent with the monomeric state. However, when PI-PLC is bound to a PC interface, three of the four residues become solvent-shielded. This shielding could occur if the residues become buried within the dimer interface or by partitioning into the membrane. The crystallographic data for wild type PI-PLC shows that Trp^{242} forms part of the barrel rim loop abutting the entrance to the active site. The pyrene derivative of W242C, as part of the rim loop, occupies a position where the Trp side chain has been proposed to insert into the bilayer (20), helping to anchor the enzyme to the membrane surface. Hence, protection of pyrene at this position from acrylamide quenching in the presence of PC vesicles would be expected. Unlike Trp^{242}, the side chains of Ser^{250} and Trp^{280} could not contact the PC interface unless PI-PLC underwent a molecular reorientation on the bilayer surface. However, this would lead to misalignment of the active site entrance, and the catalytic competence of the S250C and W280C mutants argues against this potentiality. The more plausible explanation is that these residues are buried at the protein-protein interface, as depicted in the crystal structure of the PI-PLC W47A/W242A dimer. Tyr^{57}, which is distant from the dimer interface and membrane-binding region, is freely accessible to solvent in both monomer and dimer crystal structures, consistent with the fluorescence data. Presumably, all of these Cys derivatives of PI-PLC are interfacially active because they have both Trp^{47} and Trp^{242} (or the pyrene in the case of the W242C) present as membrane anchors.

We propose a model in which the dimer interface is substantially stabilized when wild-type PI-PLC is bound to membranes. Partitioning of Trp^{47} and Trp^{242} into a PC membrane provides the primary driving force for changes in the rim loop that promote dimer formation. The rim loop is highly mobile in both mutant and wild type structures with much higher B factors than the rest of the structure, and its conformation or position can be easily changed. The proposed dimerization is a dynamic process that occurs in several steps. (i) In the absence of a membrane surface, the Trp side chains (Trp^{242} in its flexible loop as well as the helix B hydrophobic plug) sterically hinder dimer formation. (ii) At the PC membrane surface, the Trp residues partition into the membrane. (iii) This attachment of the Trp "plug" to the PC membrane allows adjacent PI-PLC molecules to approach one another while bound to the membrane interface. (iv) The tyrosine herringbone pattern forms, bringing the two monomers together on the PC interface. Dimer formation should increase the residence time of the protein on a vesicle surface and would lead to enhanced catalysis. There are likely to be other more subtle changes as well, since the enzyme when bound to PC surfaces is much more active toward water-soluble substrates (both diC_4PI and cIP) (17, 29).

REFERENCES

1. Volwerk, J. J., Shashidhar, M. S., Kuppe, A., and Griffith, O. H. (1990) *Biochemistry* **29,** 8056–8062
2. Zhou, C., Wu, Y., and Roberts, M. F. (1997) *Biochemistry* **36,** 347–355
3. Hondal, R. J., Zhao, Z., Kravchuk, A. V., Liao, H., Riddle, S. R., Yue, X., Bruzik, K. S., and Tsai, M. D. (1998) *Biochemistry* **37,** 4568–4580
4. Toker, A. (2002) *Cell Mol. Life Sci.* **59,** 761–779
5. Rebecchi, M. J., and Pentyala, S. N. (2000) *Physiol. Rev.* **80,** 1291–1335
6. Heinz, D. W., Ryan, M., Bullock, T. L., and Griffith, O. H. (1995) *EMBO J.*

14, 3855–3863
7. Heinz, D. W., Ryan, M., Smith, M. P., Weaver, L. H., Keana, J. F., and Griffith, O. H. (1996) *Biochemistry* **35,** 9496–9504
8. Moser, J., Gerstel, B., Meyer, J. E., Chakraborty, T., Wehland, J., and Heinz, D. W. (1997) *J. Mol. Biol.* **273,** 269–282
9. Essen, L. O., Perisic, O., Cheung, R., Katan, M., and Williams, R. L. (1996) *Nature* **380,** 595–602
10. Essen, L. O., Perisic, O., Katan, M., Wu, Y., Roberts, M. F., and Williams, R. L. (1997) *Biochemistry* **36,** 1704–1718
11. Heinz, D. W., Essen, L.-O., and Williams, R. L. (1998) *J. Mol. Biol.* **275,** 635–650
12. Wu, Y., Perisic, O., Williams, R. L., Katan, M., and Roberts, M. F. (1997) *Biochemistry* **36,** 11223–11233
13. Roberts, M. F., Wu, Y., Perisic, O., Williams, R. L., and Katan, M. (1998) *Am. Chem. Soc. Symp. Ser.* **718,** 137–157
14. Zhou, C., Horstman, D., Carpenter, G., and Roberts, M. F. (1999) *J. Biol. Chem.* **274,** 2786–2793
15. Lewis, K., Garigapati, V., Zhou, C., and Roberts, M. F. (1993) *Biochemistry* **32,** 8836–8841
16. Zhou, C., and Roberts, M. F. (1998) *Biochemistry* **37,** 16430–16439
17. Zhou, C., Qian, X., and Roberts, M. F. (1997) *Biochemistry* **36,** 10089–10097
18. Qian, X., Zhou, C., and Roberts, M. F. (1998) *Biochemistry* **37,** 6513–6522
19. Henrickson, H. S., and Hendrickson, E. K. (1999) *Biochim. Biophys. Acta* **1440,** 107–117
20. Feng, J., Wehbi, H., and Roberts, M. F. (2002) *J. Biol. Chem.* **277,** 19867–19875
21. Feng, J., Bradley, W., and Roberts, M. F. (2003) *J. Biol. Chem.* **278,** 24651–24657
22. Jones, S., and Thornton, J. M. (1996) *Proc. Natl. Acad. Sci. U. S. A.* **93,** 13–20
23. Hu, M. L. (1994) *Methods Enzymol.* **233,** 380–385
24. Otwinowski, Z., and Minor, W. (1997) *Methods Enzymol.* **276,** 307–326
25. Kissinger, C. R., Gehlhaar, D. K., and Fogel, D. B. (1999) *Acta Crystallogr. Sect. D* **55,** 484–491
26. Jones, T. A., and Kjeldgaard, M. (1992) *O: The Manual*, Uppsala Software Factory, Uppsala, Sweden
27. Brünger, A. T., Adams, P. D., Clore, G. M., DeLano, W. L., Gros, P., Grosse-Kunstleve, R. W., Jiang, J. S., Kuszewski, J., Nilges, M., Pannu, N. S., Read, R. J., Rice, L. M., Simonson, T., and Warren, G. L. (1998) *Acta Crystallogr. Sect. D* **54,** 905–921
28. DeLano, W. L. (2002) *The PyMOL Molecular Graphics System*, DeLano Scientific, San Carlos, CA
29. Wehbi, H., Feng, J., Kolbeck, J., Ananthanarayanan, B., Cho, W., and Roberts, M. F. (2004) *Biochemistry* **42,** 9374–9382
30. Cho, W., Bittova, L., and Stahelin, R. V. (2001) *Anal. Biochem.* **296,** 153–161
31. Apiyo, D., Zhao, L., Tsai, M.-D., and Selby, T. L. (2005) *Biochemistry* **44,** 9980–9989
32. Zhang, X., Wehbi, H., and Roberts, M. F. (2004) *J. Biol. Chem.* **279,** 20490–20500
33. Lakowicz, J. (1999) *Principles of Fluorescence Spectroscopy*, pp. 248–249, Springer, New York
34. Dekker, N., Tommassed, J., Lustig, A., Rosenbusch, J. P., and Verheij, H. M. (1997) *J. Biol. Chem.* **272,** 3179–3184
35. Snijder, H. J., Ubarretxena-Belandia, L., Blaauw, M., Kalk, K. H., Verheij, H. M., Egmond, M. R., Dekker, N., and Dijkstra, B. W. (1999) *Nature* **401,** 717–721
36. Bahnson, B. J. (2005) *Arch. Biochem. Biophys.* **433,** 96–106
37. Singer, A. U., Waldo, G. L., Harden, T. K., and Sondek, J. (2002) *Nat. Struct. Biol.* **9,** 32–36
38. Ilkaeva, O., Kinch, L. N., Paulssen, R. H., and Ross, E. M. (2002) *J. Biol. Chem.* **277,** 4292–4300
39. Zhang, Y., Vogel, W. K., McCullar, J. S., Greenwood, J. A., and Filtz, T. M. (2006) *Mol. Pharmacol.* **70,** 860–868
40. Jones, S., and Thornton, J. M. (1995) *Prog. Biophys. Mol. Biol.* **63,** 31–65

Dimer Structure of an Interfacially Impaired Phosphatidylinositol-specific Phospholipase C

Chenghua Shao, Xiaomeng Shi, Hania Wehbi, Carlo Zambonelli, James F. Head, Barbara A. Seaton and Mary F. Roberts

J. Biol. Chem. 2007, 282:9228-9235.
doi: 10.1074/jbc.M610918200 originally published online January 9, 2007
